Climatic Change
DOI 10.1007/s10584-013-0756-x

ENSEMBLES-based assessment of regional climate effects in Luxembourg and their impact on vegetation

K. Goergen · J. Beersma · L. Hoffmann · J. Junk

Received: 2 October 2012 / Accepted: 26 March 2013

Abstract Projected future regional climate changes in Luxembourg are assessed based on a six-member ensemble of regional climate models (RCM) from the ENSEMBLES project. The key aspects are projected changes in air temperature and their impacts on vegetation. Up to now, there have been only few assessments of future climate conditions for Luxembourg. As agriculture is the dominant land use in Luxembourg, possible effects on crops and vegetation in general are highly relevant. Different RCMs at 25 km spatial and a daily temporal resolution, ranging from 1961 to 2100 based on the SRES A1B emission scenario are used. To reduce systematic biases in the RCM-derived time series, a bias correction is applied. Multi-model annual mean temperatures are projected to increase by 3.1 °C between the reference time span (1961 to 1990) and the far future (2069 to 2098). Clear change signals are found in seasonal bivariate frequency distributions of air temperature and precipitation. Derived impacts are an elongation of the thermal vegetation period by 6.2 days per decade due to an earlier onset in spring; growing degree day sums show a substantial increase leading to potentially better growth conditions; the earlier onset of the vegetation period causes an increase in late frost risk, especially in the near future (2021 to 2050) projections compared to the reference period.

K. Goergen · L. Hoffmann · J. Junk
Département Environnement et Agro-Biotechnologies, Centre de Recherche Public – Gabriel Lippmann, 41, rue du Brill, 4422 Belvaux, Luxembourg

L. Hoffmann
e-mail: hoffmann@lippmann.lu

J. Junk
e-mail: junk@lippmann.lu

K. Goergen (✉)
Meteorological Institute, University of Bonn, Auf dem Hügel 20, 53121 Bonn, Germany
e-mail: k.goergen@uni-bonn.de

J. Beersma
Climate Services, Royal Netherlands Meteorological Institute (KNMI), P.O. Box 201, 3730 AE De Bilt, The Netherlands
e-mail: jules.beersma@knmi.nl

Published online: 02 May 2013

1 Introduction

Situated in Western Europe, Luxembourg covers an area of 2,590 km^2 (Fig. 1) and is characterized by a temperate semi-oceanic climate with mild winters and moderate summers.

The long-term annual mean air temperature (1971 to 2000) for the Luxembourg Findel airport SYNOP station is 8.7 °C. The warmest months are July and August with a long-term mean temperature of 17.5 °C and 17.3 °C (Table 1). Monthly mean air temperature time series of this 30-year period show positive trends for each individual month. The strongest increase can be observed for the months from March until May. Overall the increase of the annual mean air temperature is 0.5 °C per decade between 1971 and 2000.

Drogue et al. (2005) show positive trends of maximum and minimum air temperature for the second half of the 20th century for Luxembourg. Pfister et al. (2004) reveal increasing winter rainfall amounts caused by higher frequency of westerly circulation types for the same time span. Hooijer et al. (2004) and Drogue et al. (2004) investigate the impacts of climate change primarily on hydrology, based e.g. on a statistical downscaling approach. Despite such existing regional climate change studies for central Europe and the availability of regional climate model (RCM) projections (e.g. Christensen and Christensen 2007; Jacob et al. 2008), potential future climate changes and their impacts on vegetation are still missing for Luxembourg. Due to the small size of the country and because responses of plant communities, specific plants or crops responses cannot be linked to projected global or large-scale changes, regional climate change information from a downscaling of global climate model (GCM) outputs is necessary (Walther et al. 2002). Many studies indicate that

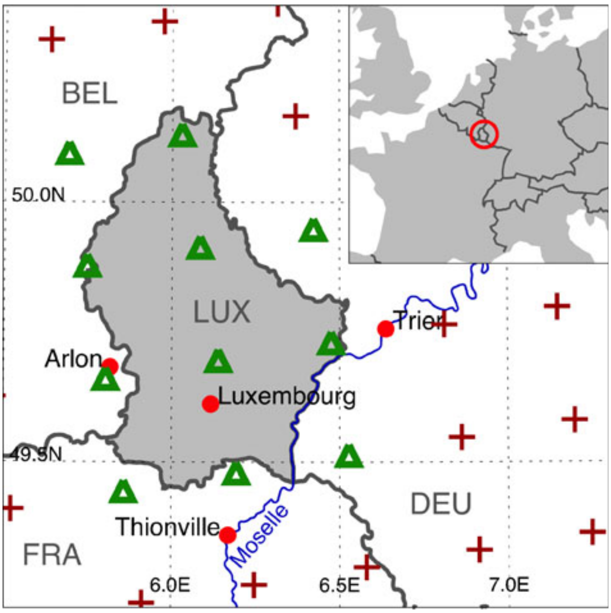

Fig. 1 Study area. *Red/green crosses/triangles*: RCM grid with a spatial resolution of 25 km (shown here is the grid of M3), grid elements used to derive the time series for Luxembourg are highlighted as *green triangles*; grid elements that overlap with Luxembourg were selected. *Red dots* mark major cities in the area. *Inset*: Luxembourg's location within Europe

Table 1 30-year (1971 to 2000) long-term monthly mean air temperatures and precipitation amounts derived from daily Findel airport SYNOP station (Luxembourg) observations. The last column shows the long-term annual values

	Jan.	Feb.	Mar.	Apr.	May	Jun.	Jul.	Aug.	Sep.	Oct.	Nov.	Dec.	Year
Temperature [°C]													
Mean	0.6	1.4	4.7	7.7	12.4	15.1	17.5	17.3	13.5	8.9	4.0	1.8	8.7
Standard deviation	2.5	2.3	1.9	1.4	1.8	1.5	2.0	1.6	1.6	1.5	1.6	1.6	6.3
Precipitation [mm month^{-1}]													
Mean	72	57	67	57	79	79	72	64	72	82	78	85	864
Standard deviation	48	40	35	39	43	49	39	31	35	51	34	49	9.3

global warming causes consistent patterns of changes in many ecosystems, e.g. shifts in phenological phases of plants or an elongation of the vegetation period (Sparks and Menzel 2002; Chmielewski et al. 2004; Estrella et al. 2007). The projected future air temperature changes will furthermore have strong impacts on crops, pests and insects (Estrella et al. 2007; Junk et al. 2012; Parmesan 2007).

Six model realisations from a dynamical downscaling approach of the ENSEMBLES project (van der Linden and Mitchell 2009) make up our ensemble of RCMs and cover the time span from 1961 to 2100. The bandwidth of the possible future regional climate developments gives thereby an indication of the associated uncertainties (Stainforth et al. 2005).

Goals of our study are a) the assessment of projected regional climate changes in Luxembourg based on a RCM ensemble with a focus on air temperature (Section 3.1 and 3.2) and precipitation (Section 3.2) and b) the investigation of the impacts of those changes on vegetation with regard to the onset and the duration of the vegetation period (Section 4.1), growing degree day sums (Section 4.2) and spring frost risk (Section 4.3).

2 Data and methods

2.1 Observational datasets

Measurements of daily air temperature from the Findel airport SYNOP station (WMO station ID=06590) are used as the regional reference time series. The station is located southeast of the City of Luxembourg (Fig. 1) and is the only official WMO station in Luxembourg.

As a basis for the bias correction of the RCM data (Section 2.2), daily mean air temperature and total precipitation of sub basin-averaged observational data have been provided by the International Commission for Hydrology of the Rhine basin (CHR) (Krahe et al. 2004; Te Linde et al. 2008), hereafter abbreviated as CHR-OBS. The overlapping model catchments are intersected with the national border of Luxembourg. Representative daily air temperature and precipitation time series for Luxembourg are derived through an area weighted spatial interpolation from the polygon-based time series.

2.2 Regional climate change projections

We use results from six transient RCM simulations from 1961 to 2098, that were all run as part of the same experiment design of the ENSEMBLES project Research Theme 2B (van der Linden and Mitchell 2009) to dynamically downscale GCM simulations. An overview is given in Table 2. The RCM results were retrieved from the ENSEMBLES data repository at the Danish Meteorological Institute (http://ensemblesrt3.dmi.dk, 2013-02-23).

Our ensemble encompasses three different GCMs and five RCMs. All GCM-RCM modeling chains are driven by the Special Report on Emission Scenarios (SRES) A1B emission scenario (Nakićenović and Swart 2000).

Van Pelt et al. (2012) show that these six GCM-RCM combinations cover similar ranges of change signals of precipitation and air temperature as those in an ensemble of overall 13 Coupled Model Intercomparison Project Phase 3 (CMIP3) GCM simulations. Sources of uncertainties in the RCM projections are a combination of the emission scenarios, the GCM model configuration, the regional climate downscaling configuration, its internal variability, e.g. of the RCM, the downscaling method itself as well as the geographic region (Giorgi 2005). Similarly to Ylhäisi et al. (2010) no weighing scheme is applied to the different models. The reference period is defined from 1961 to 1990 (currently valid WMO climate normal period), the near future is from 2021 to 2050 and the far future from 2069 to 2098 as the HadCM3-driven RCM temporal coverage ends in November and December 2099, respectively. Variables retrieved are daily mean, minimum and maximum air temperature as well as daily precipitation.

Daily time series of spatial means are extracted for each RCM from all grid cells on the respective model output grid that overlap with the area of Luxembourg (Fig. 1, green triangles). They are averaged using a weighting factor per grid element, determined by the respective overlap area.

Most of our investigated impacts on vegetation are threshold-driven; therefore absolute values are needed instead of relative changes. As the RCM outputs are biased towards observed fields (Piani et al. 2010), we follow the example of previous impact studies e.g. Junk et al. (2012) and correct the systematic biases of the RCMs towards observational reference data.

A linear bias correction scheme according to Lenderink et al. (2007) is used for daily air temperature time series and a non-linear scheme, introduced by Leander et al. (2008) and applied by Te Linde et al. (2008) to RCM data for the Rhine River basin, for precipitation. The resulting RCM-derived daily time series for Luxembourg are based on a data set, which is bias-corrected using the CHR-OBS hydrometeorological reference data set for the reference period from 1961 to 1990.

2.3 Basic definitions for the impact analyses

Air temperature often plays a dominant role in phenological studies as it affects the rate of most of the plant's chemical and biological processes. The thermal vegetation period as used

Table 2 Regional climate change projection datasets used by the study. Given are the model abbreviations in the text, the driving GCM, the RCM used for the downscaling, and the institution, that ran the RCM. All GCMs are based on the SRES A1B emission scenario. RCM data spatial resolution: 25 km×25 km; temporal resolution: daily means and totals; time span: 1961 to 2098

Model abbreviation	GCM	RCM	Institution (providing the RCM data)
M1	ARPEGE	HIRHAM v5	DMI
M2	ECHAM5-r3	RACMO v2.1	KNMI
M3	ECHAM5-r3	REMO v5.7	MPI-M
M4	HadCM3Q0 (normal sensitivity)	CLM v2.4.6	ETHZ
M5	HadCM3Q3 (low sensitivity)	HadRM v3.0	Hadley Centre
M6	HadCM3Q16 (high sensitivity)	HadRM v3.0	Hadley Centre

in our analyses is according to Chmielewski and Rötzer (2001) and defined by a threshold of 5.0 °C for the daily mean air temperature that must be exceeded for at least five consecutive days; this marks the beginning of the vegetation period. The same number of days below 5 °C marks the end of the vegetation period. Using this definition, we derive the length of the vegetation period for each individual year of the analysed time span of each of the six ensemble members. The base temperature $\widehat{T}$ is set to 5 °C as plant growth is negligible below this daily mean air temperature threshold (Skaugen and Tveito 2004).

Growing degree days are a well-established measure to quantify the available energy for plant growth in general (Bonhomme 2000; Clark and Thompson 2010; Saiyed et al. 2009). To quantify the available heat during the growing season, we use growing degree day sums (GDDS) based on °C in the unit degree days [DD], calculated according to the following equation:

$$GDDS = \sum_{i=1}^{365/366} \left(T_i - \widehat{T}\right), \; T_i \geq \widehat{T} \quad \widehat{T} = 5°\mathrm{C}$$

For the GDDS the same base temperature $\widehat{T}$ is used; the GDDS can e.g. be used as a principal climate variable to rate the climatic suitability of an area for production of spring-seeded grains (Bootsma et al. 2005) in agriculture or as a climate impact indicator as e.g. in Grigorieva et al. (2010).

A frost day in our study is defined by a daily minimum air temperature below 0 °C. We defined frost risk by the cumulative sums of daily minimum air temperature below 0 °C in the first 60 days of the vegetation period derived for 30-year time spans.

3 Past and future climatic conditions

3.1 Temporal evolution of air temperature

For Luxembourg and its vicinity large-scale changes towards higher air temperatures are supposed to be more pronounced than those for precipitation according to large-scale assessments in the 4th IPCC Assessment Report (Parry et al. 2007; Solomon et al. 2007).

Figure 2 shows the annual mean air temperature values from our RCM ensemble as a multi-model bandwidth, multi-model mean and overlaid the annual means from the CHR-OBS data set. To relate these data to the local reference SYNOP station, the observations from the Findel airport SYNOP station are additionally shown.

A comparison within the reference period (1961 to 1990) of the long-term averages of the annual mean air temperature observations at the airport station (T_{mean}=8.3 °C) and the bias-corrected RCM multi-model mean control runs (T_{mean}=8.1 °C) shows a good agreement.

From 2000 onwards, the observations at the Findel airport station are on the upper end of the multi-model bandwidth, identifying the future projections of air temperature change based on the A1B greenhouse gas emission scenario as an optimistic estimation for the first decade of the 21st century for the area of Luxembourg.

The 30-year long-term averages of the multi-model annual mean temperatures increase steadily from 8.1 °C in the reference period (1961 to 1990) to 9.5 °C in the near (2021 to 2050) and 11.2 °C in the far future (2069 to 2098). These temperature increases are comparable with the findings of Jacob et al. (2008) for the neighbouring Germany.

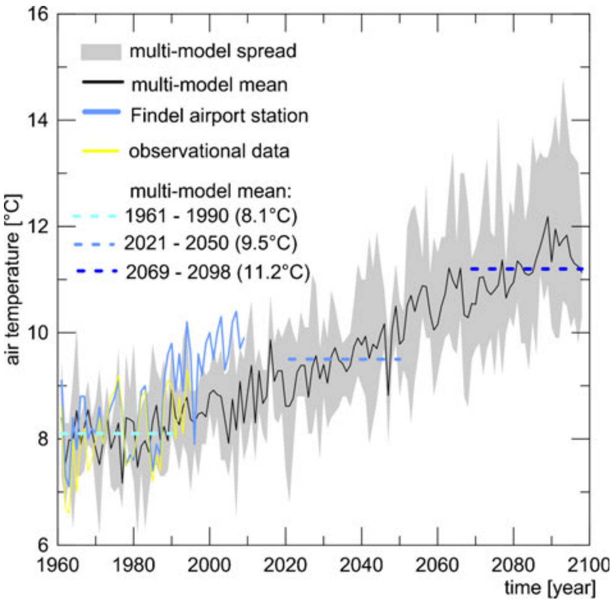

Fig. 2 Time series of annual mean air temperature. *Black line*: multi-model mean (N=6 RCMs); long-term annual mean 1961 to 1990=8.1 °C. *Grey shading*: multi-model bandwidth (minimum, maximum). *Yellow line*: CHR-OBS reference dataset; long-term annual mean 1961 to 1990=8.1 °C. *Blue line*: Findel airport SYNOP station; long-term annual mean 1961 to 1990=8.3 °C. *Blue dashed horizontal lines*: multi model means for the three 30-year analyses time spans

3.2 Bivariate frequency distributions for air temperature and precipitation

In order to conjointly analyse the projected changes in air temperature and precipitation, bivariate absolute frequency distributions are calculated for the meteorological summer (JJA) and winter (DJF) seasons for the three analysis time spans (Fig. 3). The figure is based on daily means of air temperature and daily totals of precipitation per time span (i.e. 30 years×90 days (or 91 days in a leap year) per season) and is created as follows: (1) values below 0.5 mm d^{-1} in the precipitation time series per RCM are recoded to 0.0 mm d^{-1}; (2) an arithmetic multi-model mean is calculated from the six ensemble members for air temperature and precipitation; (3) again a re-classification sets all precipitation values below 1.0 mm d^{-1} to 0.0 mm d^{-1}; (4) both, air temperature and precipitation, are classified with a class range of 1 °C and 1 mm d^{-1} for the meteorological winter and summer seasons. Please note that extreme values in the distributions of Fig. 3 do not occur due to the calculation of the multi-model mean in step 2.

Comparing the near and far future time spans with the reference period, a clear shift of air temperature towards higher values in the near and far future can be observed for both seasons. This shift is more pronounced in summer. The maximum of the frequency distribution during summer shifts from 16 °C and 2 mm d^{-1} in the reference time span to 17 °C and 1 mm d^{-1} in the near and 20 °C and 1 mm d^{-1} in the far future. The results for both variables are in line with the expected changes as described e.g. by Christensen and Christensen (2007) or van der Linden and Mitchell (2009) for central Europe.

Precipitation shows a distinct decrease during the summer months, especially in the far future (Fig. 3c). Contrasting to this, there is a comparatively moderate precipitation increase

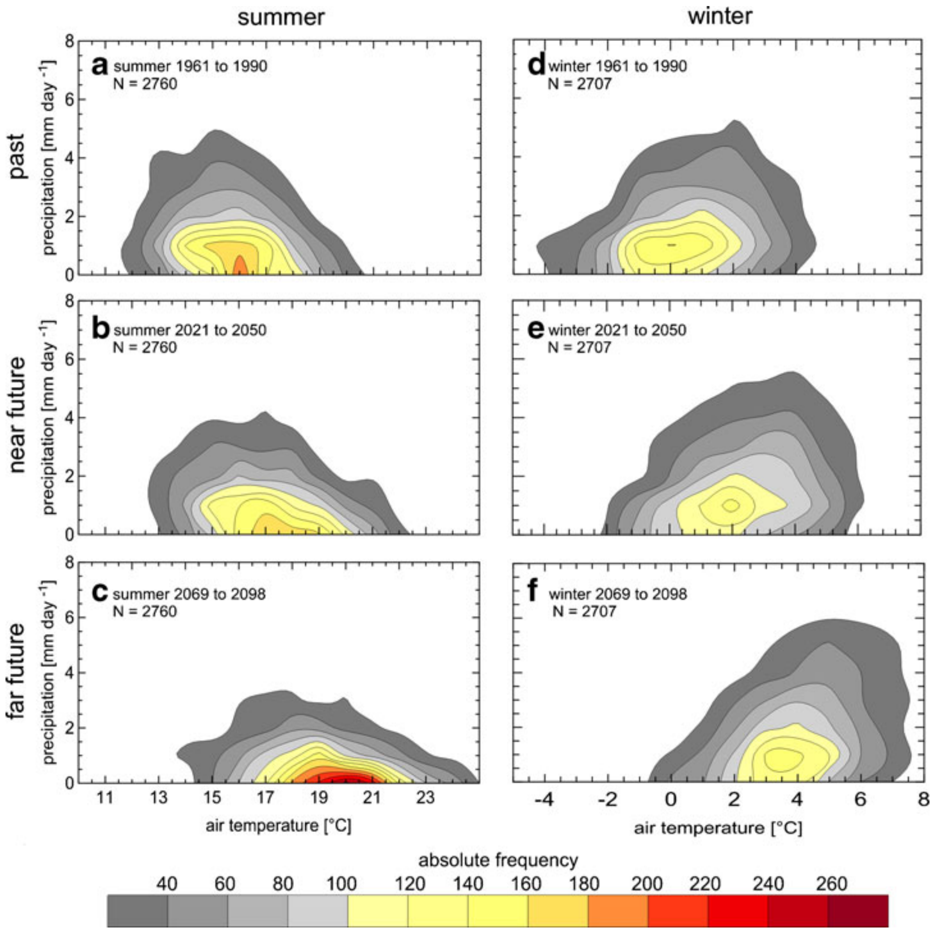

Fig. 3 Bivariate absolute frequency distribution of daily mean air temperature [°C] and daily total precipitation [mm d^{-1}] of multi-model means (*N*=6 RCMs) for the reference time span (**a**, **d**: 1961 to 1990) and the near (**b**, **e**: 2021 to 2050) and far future (**c**, **f**: 2069 to 2098) for meteorological summer (*left*) and winter (*right*). Base data are classified with a class range of 1 °C for air temperature and 1 mm d^{-1} for precipitation

during the winter season. These changes may be caused by modified large-scale flow patterns over the North Atlantic (van Ulden and van Oldenborgh 2006). It should be noted that in Fig. 3 two RCM output variables with different levels of uncertainties are combined. Precipitation simulations in the GCM and RCM control runs show in comparison to observations a much higher level of uncertainty than air temperature simulation results.

4 Impacts on vegetation

4.1 Change of the vegetation period

The impacts of the climatic changes on the vegetation period are quantified based on a thermal definition (see Section 2.3).

Figure 4 shows the duration of the vegetation period in days as a multi-model bandwidth and multi-model mean; the observational data set from the Findel SYNOP station is also included in the figure. On the right y axis the beginning and the end of the vegetation period is displayed in day of the year (DOY) as a multi-model mean with linear regression curves overlaid. The durations of the vegetation period derived for the reference period (1961 to 1990) from the Findel airport station time series (mean duration: 249 days) as well as from the CHR-OBS dataset (240 days) are within the six-ensemble member spread (multi-model mean duration: 243 days). Rötzer and Chmielewski (2001) show an average length of the vegetation period for southern England and northern Germany of 210 days for the time span from 1961 until 1998.

For the whole time span from 1961 to 2098, an elongation of the vegetation period of 6.2 days per decade can be identified. This elongation is caused by an earlier onset of the vegetation period in spring of 3.8 days per decade and a later end in autumn of 2.4 days per decade. Our findings for Luxembourg are in line with those of Chmielewski et al. (2005) for Saxony (Germany) who also attribute the elongation of the vegetation period mainly to an earlier onset in spring. Menzel et al. (2006) show an average advance of phenological phases in spring for Europe of 2.5 days per decade for the period from 1971 until 2000. In comparison, for the same time span the onset of the vegetation period is 1.6 days per decade earlier in Luxembourg, derived from the Findel airport station time series.

4.2 Change of the growing degree day sums

The GDDS can be used as an indicator for the available energy for the growth of the plants during the vegetation period (Grigorieva et al. 2010).

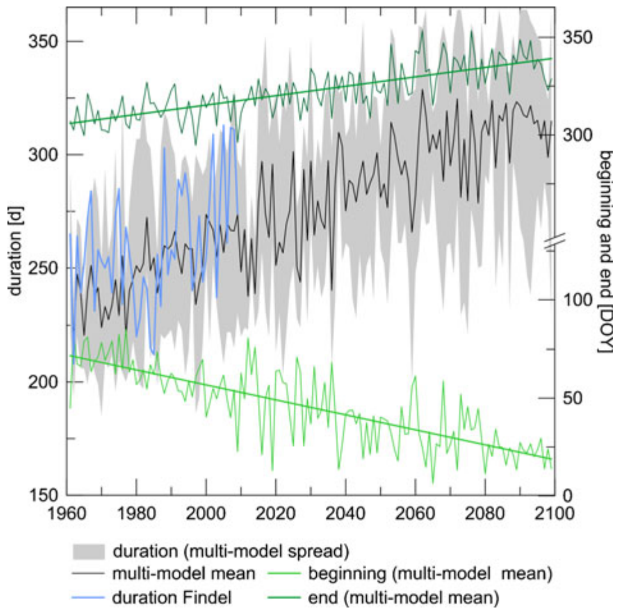

Fig. 4 Time series of vegetation period length, its beginning and end. Left y axis: duration of vegetation period [d] per year as defined by Chmielewski and Rötzer (2001). *Black line*: multi-model mean of RCM ensemble; *grey shading*: multi-model bandwidth (minimum, maximum); *blue line*: Findel airport station. Right y axis: multi-model mean of RCM ensemble of beginning (*light green*) and end (*dark green*) of vegetation period [DOY] with linear regression functions fitted

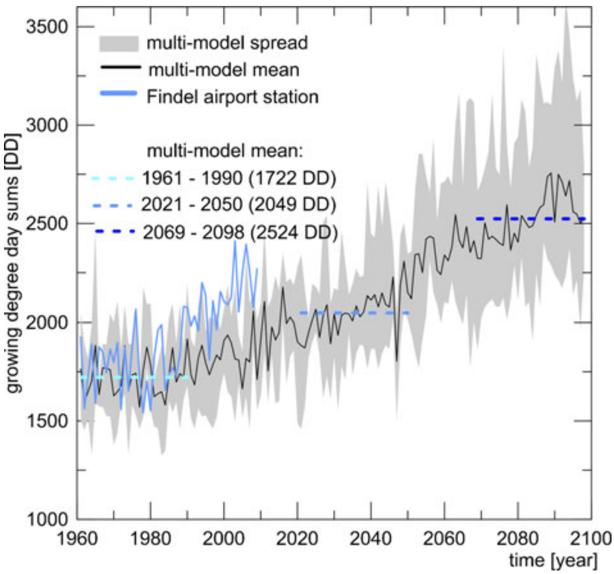

Fig. 5 Time series of yearly growing degree day sums (GDDS) [DD] accumulated during the vegetation period. *Black line*: multi-model mean of RCM ensemble; *grey shading*: multi-model bandwidth (minimum, maximum); *blue line*: Findel airport SYNOP station with a GDDS long-term annual mean 1961 to 1990= 1798 DD. *Blue dashed horizontal lines*: multi-model means for the three 30-year analyses time spans

The GDDS within the vegetation periods show a continuous increase with a clear change signal (Fig. 5). The multi-model mean spans thereby a range from a minimum of 1569 DD to a maximum of 1917 DD during the reference period. In the near future they range from 1802 DD to 2309 DD and from 2322 DD to 2757 DD in the far future, which is a considerable increase. As long as other factors that may limit plant growth (e.g. precipitation, nutrient supply) are not negatively affected, this leads to an advanced timing of phenophases in general.

4.3 Change of spring frost risk

Frost damages are a large economic risk for agriculture and especially horticulture. Most harmful events occur shortly before or during the plant's bloom stage; thereby severe frost events lead often to a substantial reduction in crop yields, while light frosts often only degrade the harvest's quality (Eccel et al. 2009). With the general tendency towards an earlier onset of the vegetation period (Fig. 4) and the associated earlier flowering dates in the future, this might lead to an increased exposure of plants to damages due to late frost events.

We assume that the future change in the number of frost days at the beginning of the vegetation period during spring can be used as an indicator for an altered late frost risk imposed on plants and crops. Hence, we analysed the first 60 days of each individual vegetation period in our 30-year analysis period to assess this potential frost risk for each RCM in the ensemble separately.

Each line in Fig. 6 represents the cumulative sum of all negative air temperatures, i.e. a daily minimum temperature below 0 °C, in the first 60 days of the vegetation period for 30-year time span for each ensemble member (M1 to M6) shown as 30-year averages. Two out of the six models (M1 and M5) show lower cumulative temperature sums for the future time spans. The other four models show considerable changes towards higher negative air temperature sums. This we interpret as a change towards an increased late frost risk in the future.

The absolute number of frost days for the three analyses time spans is given in Fig. 7 as a multi-model mean of frost days of all ensemble members. Based on the daily minimum air temperature time series, the number of frost days for each ensemble member and each vegetation period is calculated. Afterwards, the ensemble's average of the number of frost days is derived. The differences in the number of frost days between the reference period and the near future is statistically significant (P=0.05), the differences between the reference period and the far future are not. Similarly to Figs. 2, 4 and 5, the spread of the number of frost days gives an indication of the range of the change signals of the RCMs in our ensemble, which is also reflected in the differences of the model behaviour in Fig. 6.

In the near future our six RCM ensemble members project a tendency towards more frost events at the beginning of the vegetation period. The risen daily mean air temperatures in the projections lead to the earlier vegetation period onset, but still frost days occur. The situation changes in the far future, where the frequency of days with frost decreases as compared to the near future. The continued air temperature increase leads to less frequent days with frost at the beginning of the vegetation period, but the higher variability still leads to more frost days than in the past reference period.

Based on these results, there is an increased risk for late frost induced damage of vegetation in Luxembourg in the near and the far future as compared to the current World Meteorological Organisation climate normal period from 1961 to 1990.

5 Summary

Based on an ensemble of bias-corrected regional climate change projections extracted for the area of Luxembourg from ENSEMBLES RCM simulations, changes of near and far future

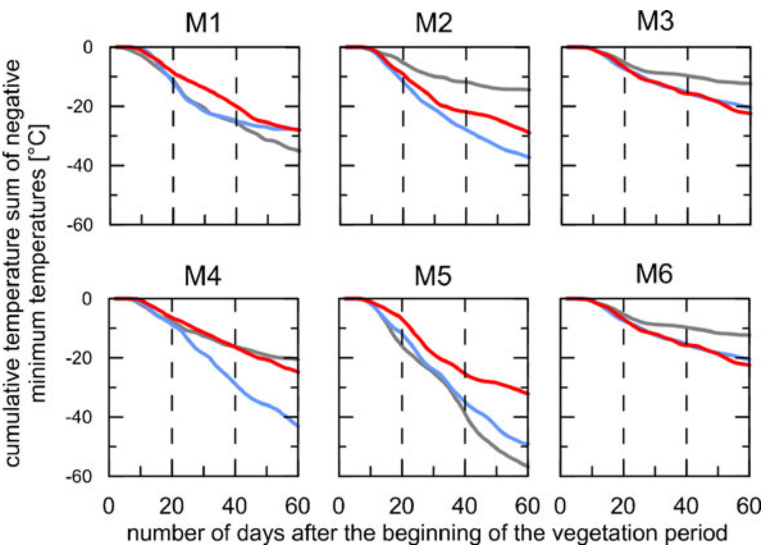

Fig. 6 Cumulative sums of daily minimum near surface temperature below 0 °C in the first 60 days of the vegetation period derived for 30-year time spans, 30-year averages are shown; *grey line*: 1961 to 1990; *blue line*: 2021 to 2050 and *red line*: 2069 to 2098

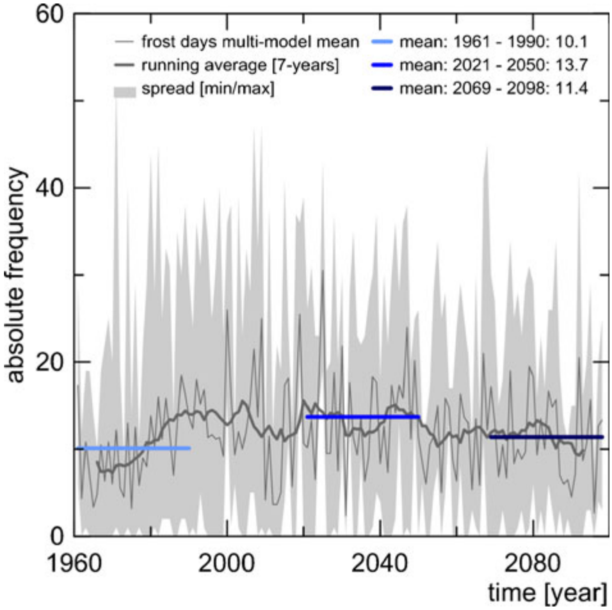

Fig. 7 Time series of average number of frost days during the first 60 days of the vegetation period. *Grey thin line*: multi-model mean of frost days; *thick grey line*: 7-years running average; *grey shading*: multi-model bandwidth (minimum, maximum). *Blue horizontal lines*: multi-model means for the three 30-year analyses time spans

air temperature and precipitation are analysed. Accompanied by an increasing bandwidth of the RCM ensemble, there is a steady increase in the 30-year long-term averages of the multi-model annual mean temperatures of 3.1 °C from the reference time span to the far future.

Bivariate absolute frequency distributions of air temperature and precipitation for meteorological summer and winter seasons show clear tendencies towards higher air temperatures as well as a distinct decrease of precipitation during summer but a moderate increase during winter.

Tendencies of change are homogeneous among the ensemble members, although very different GCM-RCM combinations are used.

The length of the thermal vegetation period in Luxembourg increases by 6.2 days per decade, mainly due to an earlier onset in spring. The growing degree day sum is used to analyse the air temperature's effect on vegetation during the vegetation period. We find a considerable increase from a 30-year multi-model mean average of 1722 DD in the reference time span to 2524 DD in the far future, which means better growth conditions in combination with the elongated vegetation period, albeit only when these factors are considered alone.

If we anticipate earlier flowering dates – linked to the aforementioned changes –, we find an increase in late frost risk during the beginning of the vegetation period. In the near future there is an increase of such events in relation to the reference period from 1961 to 1990 as the raised temperatures change the vegetation period, which does not exclude potentially harmful frost events. This development is weakened in the far future, but still a higher risk persists than during the reference period.

Acknowledgments The RCM simulation results were produced in the framework of the ENSEMBLES project (http://ensembles-eu.metoffice.com) Research Theme 2B and made available through the data portal of the Danish Meteorological Institute (DMI) (http://ensemblesrt3.dmi.dk). The CHR-OBS hydrometeorological reference dataset has been provided by the International Commission for the Hydrology of the Rhine Basin (CHR) (http://www.chr-khr.org) in the context of its RheinBlick2050 project. In situ meteorological observations for the Findel airport station in Luxembourg were provided by the Service Météorologique of the airport administration. The scientific research presented in this publication has been given financial support by the National Research Fund of Luxembourg through grant FNR C09/SR/16 (project "CLIMPACT"); furthermore, parts of the study were financially supported by the REMOD projects of the Centre de Recherche Public – Gabriel Lippmann.

References

Bonhomme R (2000) Bases and limits to using 'degree day' units. Eur J Agron 13:1–10

Bootsma A, Gameda S, McKenney SDW (2005) Impacts of potential climate change on selected agroclimatic indices in Atlantic Canada. Can J Soil Sci 85:329–343

Chmielewski FM, Rötzer T (2001) Response of tree phenology to climate change across Europe. Agric For Meteorol 108:101–112

Chmielewski FM, Müller A, Ekko B (2004) Climate change and trends in phenology of fruit trees and field crops in Germany, 1961–2000. Agric For Meteorol 121:69–78

Chmielewski FM, Müller A, Küchler W (2005) Possible impacts of climate change on natural vegetation in Saxony (Germany). Int J Biometeorol 50:96–104

Christensen J, Christensen O (2007) A summary of the PRUDENCE model projections of changes in European climate by the end of this century. Clim Chang 81:7–30

Clark RM, Thompson R (2010) Predicting the impact of global warming on the timing of spring flowering. Int J Climatol 30:1599–1613

Drogue G, Pfister L, Leviandier T, Idrissi E, Iffly JF, Matgen P, Humbert J, Hoffmann L (2004) Simulating the spatio-temporal variability of streamflow response to climate change scenarios in a mesoscale basin. J Hydrol 293:255–269

Drogue G, Mestre O, Hoffmann L, Iffly JF, Pfister L (2005) Recent warming in a small region with semi-oceanic climate, 1949–1998: what is the ground truth? Theor Appl Climatol 81:1–10

Eccel E, Rea R, Caffarra A, Crisci A (2009) Risk of spring frost to apple production under future climate scenarios: the role of phenological acclimation. Int J Biometeorol 53:273–286

Estrella N, Sparks TH, Menzel A (2007) Trends and temperature response in the phenology of crops in Germany. Glob Chang Biol 13:1737–1747

Giorgi F (2005) Climate change prediction. Clim Chang 73:239–265

Grigorieva EA, Matzarakis A, de Freitas CR (2010) Analysis of growing degree-days as a climate impact indicator in a region with extreme annual air temperature amplitude. Clim Res 42:143–154

Hooijer A, Klijn F, Pedroli GBM, Van Os AG (2004) Towards sustainable flood risk management in the Rhine and Meuse river basins: synopsis of the findings of IRMA-SPONGE. River Res Appl 20:343–357

Jacob D, Göttel H, Kotlarski S, Lorenz P, Sieck K (2008) Klimaauswirkungen und Anpassung in Deutschland – Phase 1: Erstellung regionaler Klimaszenarien für Deutschland. Umweltbundesamt Forschungsbericht 204 41 138 (UBA-FB 000969), 159 pp

Junk J, Eickermann M, Görgen K, Beyer M, Hoffmann L (2012) Ensemble-based analysis of regional climate change effects on the cabbage stem weevil (Ceutorhynchus pallidactylus (Mrsh.)) in winter oilseed rape (Brassica napus L.). J Agric Sci 150:191–202

Krahe P, Herpertz D, Eberle M, Busch N, Buiteveld H, Naef F, Helbig A, Beersma J (2004) Development of methodologies for the analysis of the efficiency of flood reduction measures in the Rhine basin on the basis of reference floods. CHR Report I-21, Lelystad, 57 pp

Leander R, Buishand TA, van den Hurk BJJM, de Wit MJM (2008) Estimated changes in flood quantiles of the river Meuse from resampling of regional climate model output. J Hydrol 351:331–343

Lenderink G, Buishand TA, Van Deursen W (2007) Estimates of future discharges of the river Rhine using two scenario methodologies: direct versus delta approach. Hydrol Earth Syst Sci 11:1145–1159

Menzel A, Sparks TH, Estrella N, Koch E, Aasa A, Ahas R, Alm-Kübler K, Bissolli P, Braslavská O, Briede A, Chmielewski FM, Crepinsek Z, Curnel Y, Dahl Å, Deflila C, Donnelly A, Filella Y, Jatczak K, Måge F, Mestre A, Nordli Ø, Penuelas P, Pirinen P, Remišová V, Scheifinger H, Striz M, Susnik A, van Vliet AJH, Wielgolaski FE, Zach S, Zust A (2006) European phenological response to climate change matches the warming pattern. Glob Chang Biol 12:1969–1976

Nakićenović N, Swart R (eds) (2000) Special report on emissions scenarios: a special report of Working Group III of the Intergovernmental Panel on Climate Change. Cambridge University Press, Cambridge, 570 pp

Parmesan C (2007) Influences of species, latitudes and methodologies on estimates of phenological response to global warming. Glob Chang Biol 13:1860–1872

Parry ML, Canziani OF, Palutikof JP, van der Linden JP, Hanson CE (eds) (2007) Climate change 2007: impacts, adaptation and vulnerability. Contribution of Working Group II to the fourth assessment report of the Intergovernmental Panel on Climate Change. Cambridge University Press, Cambridge, 976 pp

Pfister L, Drogue G, El Idrissi A, Iffly JF, Poirier C, Hoffmann L (2004) Spatial variability of trends in the rainfall-runoff relationship: a mesoscale study in the Mosel basin. Clim Chang 66:67–87

Piani C, Haerter JO, Coppola E (2010) Statistical bias correction for daily precipitation in regional climate models over Europe. Theor Appl Climatol 99:187–192

Rötzer TF, Chmielewski FM (2001) Phenological maps of Europe. Clim Res 18:249–257

Saiyed IM, Bullock PR, Sapirstein HD, Finlay GJ, Jarvis CK (2009) Thermal time models for estimating wheat phenological development and weather-based relationships to wheat quality. Can J Plant Sci 89:429–439

Skaugen TE, Tveito OE (2004) Growing-season and degree-day scenario in Norway for 2021–2050. Clim Res 26:221–232

Solomon S, Qin D, Manning M, Chen Z, Marquis M, Averyt KB, Tignor M, Miller HL (eds) (2007) Climate change 2007: The physical science basis. Contribution of Working Group I to the fourth assessment report of the Intergovernmental Panel on Climate Change. Cambridge University Press, Cambridge, 996 pp

Sparks TH, Menzel A (2002) Observed changes in seasons: an overview. Int J Climatol 22:1715–1725

Stainforth DA, Aina T, Christensen C, Collins M, Faull N, Frame DJ, Kettleborough JA, Knight S, Martin A, Murphy JM, Piani C, Sexton D, Smith LA, Spicer RA, Thorpe AJ, Allen MR (2005) Uncertainty in predictions of the response to rising levels of greenhouse gases. Nature 433:403–406

Te Linde AH, Aerts JCJH, Hurkmans RTWL, Eberle M (2008) Comparing model performance of two rainfall-runoff models in the Rhine basin using different atmospheric forcing data sets. Hydrol Earth Syst Sci 12:943–957

van der Linden P, Mitchell JFB (2009) ENSEMBLES: climate change and its impacts: summary of research and the results from the ENSEMBLES project. Met Office Hadley Centre, Exeter, 160 pp

Van Pelt SC, Beersma JJ, Buishand TA, van den Hurk BJJM, Kabat P (2012) Future changes in extreme precipitation in the Rhine basin based on global and regional climate model simulations. Hydrol Earth Syst Sci Discuss 9:6533–6568

Van Ulden AP, van Oldenborgh GJ (2006) Large-scale atmospheric circulation biases and changes in global climate model simulations and their importance for climate change in Central Europe. Atmos Chem Phys 6:863–881

Walther GR, Post E, Convey P, Menzel A, Parmesan C, Beebee TJC, Fromentin JM, Hoegh-Guldberg O, Bairlein F (2002) Ecological responses to recent climate change. Nature 416:389–395

Ylhäisi JS, Tietäväinen H, Peltonen-Saino P, Venäläinen A, Eklund J, Räisänen J, Jylhä K (2010) Growing season precipitation in Finland under recent and projected climate. Nat Hazards Earth Syst 10:1563–1574